EVALUATION OF UNFIRED MAGNESIA CHROME BRICKS IN RH DEGASSERS: CUSTOMER PERFORMANCE

Fajardo, G. L.*[1]; Melo, B. L. B[1].; Pagliosa, C.[1]; Martins, G. G.[1]; Ávila, H. C.[1]

[1] RHI Magnesita, Contagem, Brazil

*gabriela.fajardo@rhimagnesita.com

ABTRACT

The ever-increasing demand for processes with low carbon emissions is a great challenge for the steelmaking industry. Aligned with that, an unfired magnesia chrome brick with a special binder system has been developed to replace the traditional fired material, which have been used in RH Degassers since the 1960s. This metallurgical equipment is divided into different regions: hot-off take, upper vessel, lower vessel, and snorkels. Unfired $MgO-Cr_2O_3$ bricks were used in lower vessel of different customers with good performance compared to the fired product. This work aims to evaluate the tempered $MgO-Cr_2O_3$ bricks performance and its profile after use in two Brazilians integrated mills.

1. INTRODUCTION

Initially developed to reduce the hydrogen content in molten steel, RH Degasser has been used for decarburization since the late 1970s. Nowadays, the RH process can produce steels with hydrogen content bellow 1ppm and carbon content bellow 20ppm, which is an important specification for the automotive industry[1].

A typical RH Degasser consists of hot-off take, upper vessel, lower vessel, and inlet and outlet snorkels. The snorkels are dipped into the steel ladle and inert gas (mostly argon) is injected into the inlet snorkel to lift the molten steel and starts its circulation. After that, the vessel is evacuated, and decarburization starts. At this point, oxygen blowing can be used for a forced decarburization. Depending on customers requirements, aluminum or silicon can be added deoxidize the molten steel and allow inclusion flotation. To finish this process, iron-alloys are added to reach the steel desired composition[1].

The right choice of refractory materials is important to improve RH performance. Magnesia chrome bricks are the most widely used materials in this equipment. They are known for their excellent resistance to erosion and corrosion resistance, dimensional stability at high temperatures, and low thermal expansion[2]. Fired magnesia chrome bricks are classified into three groups: direct bonded, semi-rebounded, and rebounded bricks. The first are systems without fused raw materials in their composition. On the other hand, semi-rebounded and rebounded bricks have fused raw materials in their composition, such as fused magnesia and fused magnesia-chromite[3]. The difference between the latter two is that semi-rebounded bricks have a lower content of fused raw materials than the rebounded ones[4].

Data citation: Proceeding title and author names available in the first page;

Source: Proceeding 26, XLII ALAFAR Congress, Foz do Iguaçú, Brazil, 2022

The hot off-take and the upper vessel have no contact with molten steel or slag. Their main wear mechanism is thermal shock, due to the thermal cycle during operation. To reach this application requirements, both regions are commonly lined with direct bonded bricks. The lower vessel and snorkels are exposed to severe wear mechanisms: corrosion due to interaction with the process slag, thermal shock due to several degassing cycles, and erosion due to steel recirculation[5]. These two regions are the largest refractories consumers, which are usually semi-rebounded or rebounded bricks.

Since the 1960s magnesia chrome bricks have been used in the steel industry, leading to high energy consumption by refractories makers, as their firing process is carried out at high temperatures above 1600°C. A new C-free binder system was developed, allowing the magnesia chrome bricks to be delivered to the customer only tempered at 200°C. The material fast-sintering capability enables the desired microstructure to be achieved with energy from the steelmaking process. This work aims to show the routine usage of this environmentally friendly brick under the severe chemical and thermomechanical wear mechanisms of RH Degassers.

2. DEVELOPMENT

Field trials with the tempered $MgO\text{-}Cr_2O_3$ brick have been performed in Brazilian integrated mills since 2019 and were reported in previous works[1,6,7]. Going one step further, results from routine use of the material on the lower vessel walls of two customers will be presented in this work.

2.1. Customer A

Customer A has a production volume of 2,200,000 ton/year and its RH has a circulation rate of 130 ton/min. The cross section of the RH lower vessel project is shown in Figure 1. The bricks length varies from 250 up to 350mm with the longest length being located at the outlet wall. This profile is due to the impact that the outlet wall suffers during the movement of the molten steel inside the RH vessel. Tempered $MgO\text{-}Cr_2O_3$ bricks are assembled until the 10th layer of the lower vessel wall, which is the area where the steel and slag from the process interact with the refractory lining. From there, recovered material is used.

Figure 1. Lower vessel cross section of customer A RH.

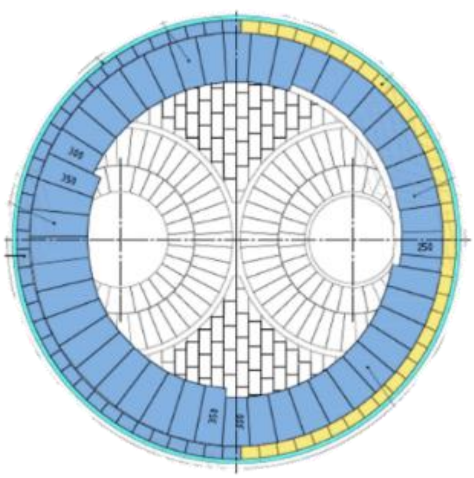

For illustration purpose, a specific campaign from customer A is presented in this work and its lower vessel ready for operation is shown in Figure 2.

Figure 2. Assembly of customer A lower vessel (a) inlet and (b) outlet side.

(a)

(b)

This vessel operated with regular process parameters: average treatment and vacuum times were about 40 and 32 min, respectively; total volume of oxygen blown during the campaign was around 760 kNm^3.

The equipment stopped with 170 heats due to the mill's planning and did not show any nonstandard occurrence. This was an outstanding result considering the RH Degasser average life of 125 heats from January until July 2022 in this mill. Figure 3 shows the vessel after operation.

Figure 3. Customer A lower vessel (a) inlet and (b) outlet sides after usage.

(a) (b)

After the vessel has been cooled down, the residual brick length (RBL) was manually measured with a measuring tape and the result for the area where the tempered MgO-Cr_2O_3 bricks were assembled is shown in Figure 4.

Figure 4. Residual brick length of customer A lower vessel.

Layer	Residual brick length													
	1	2	3	4	5	6	7	8	9	10	11	12	13	14
10	220	230	170	165	160	200	210	245	265	250	250	270	220	215
9	220	230	170	170	160	210	220	250	265	250	240	280	220	215
8	225	240	170	170	165	210	220	245	265	260	240	275	220	225
7	230	240	180	170	170	210	220	250	270	260	250	275	220	225
6	230	240	230	225	220	210	225	250	270	260	250	280	225	230
5	240	250	240	225	220	215	230	250	270	265	270	280	240	240
4	240	250	240	230	220	215	230	240	260	265	260	280	240	240
3	250	260	250	230	225	220	230	200	210	220	210	220	250	250
2	250	260	250	240	230	230	240	200	210	220	210	220	250	250
1	250	260	250	240	230	230	240	200	210	220	210	220	250	250

250

300

350

From the comparison between the initial and residual brick length, it was possible to estimate the average and maximum wear rate for each area of the lower vessel wall. The potential life was also estimated considering a safety residual length of 30mm and the maximum wear rate of each area. Table 1 summarizes these results.

Table 1. Wear rate and potential life of customer A lower vessel.

Initial brick length (mm)	Wear rate (mm/heat)		Potential life (heats)
	Average	Maximum	
250	1.42	1.47	308
300	1.43	1.77	315
350	1.53	1.65	319

The potential life results are very satisfying as the performance goal for customer A is 140 heats, indicating that the tempered $MgO\text{-}Cr_2O_3$ material is suitable for regular supply for this customer lower vessel walls.

2.2. Customer B

2.2.1. Performance

Customer B has a production volume of 4,200,000 ton/year and its RH capacity is 230 ton. This customer's standard RH project uses two grades of material in the lower vessel. A nobler material is used on the outlet side than on the inlet side. The tempered material was manufactured in the nobler grade and therefore used in the outlet side of the vessel. The material was applied up to the 15th row, where the bricks length is 300mm. Figure 5 shows the area assembled with tempered $MgO\text{-}Cr_2O_3$ bricks.

Figure 5. Assembly of customer B lower vessel outlet side.

Figures 6 to 9 show some process data from RH campaigns from January to July 2022, including the one under discussion. The average oxygen blown per heat for the campaign under analysis was 109 Nm^3, therefore within 50% of the evaluated values, as per Figure 6. The same is true for the variables average treatment time and heats per day, which are shown in Figures 7 and 8, respectively. Their values for the analyzed campaign were 26.5 minutes and 12.2 heats/day, respectively. Interstitial free (IF) steel represented 37% of production during the campaign in focus. According to Figure 9, this value is between the third and fourth quartiles. This high incidence of IF steels can be harmful to the refractory since its production process is more aggressive.

Figure 6. Average oxygen blown per heat.

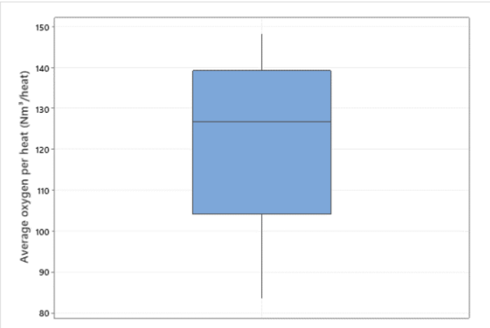

Figure 7. Average treatment time.

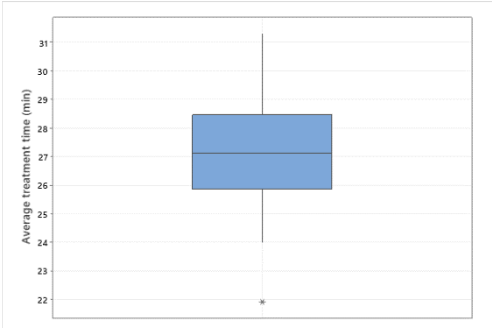

Figure 8. Vessel rhythm.

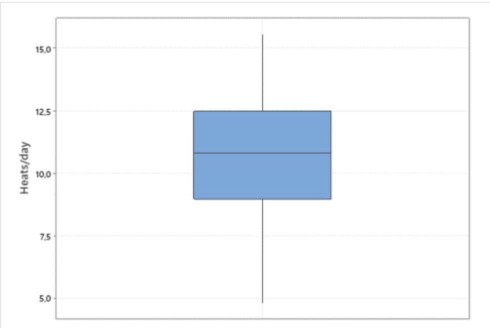

Figure 9. Interstitial free steel production.

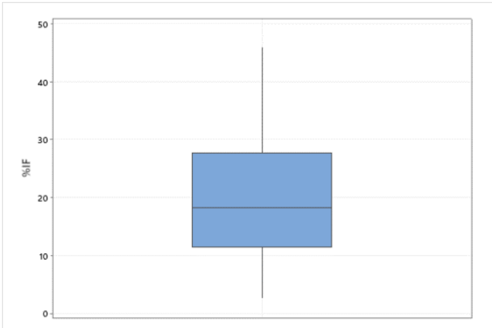

The equipment stopped with 122 heats due to the mill’s planning. Figure 10 shows the lower vessel outlet side after operation.

Figure 10. Customer B lower vessel outlet side after usage.

Figure 11 shows the residual brick length measured once the vessel was cooled down. Only the region with tempered $MgO\text{-}Cr_2O_3$ material was measured. In addition, measurement is only possible when a gap is formed between the bricks, allowing the tape measure to be inserted. The most worn area happened in the northeast side, with an RBL of 80mm. This is the area that suffers the highest impact as the molten steel circulates. A post-mortem sample was selected from this area for characterization purposes and will be further presented.

Figure 11. Residual brick length of customer B lower vessel outlet side.

Layer	Residual brick length							
	N	NE	E	SE	S	SW	W	NW
11	200	200						210
10	170	180						200
9	140	130						180
8	130	110						160
7	130	100						140
6	140	80						130
5	160	80						130
4	170	110						180
3	220							230
2	220							
1	220							

From the RBL result it was possible to calculate the average and maximum wear of the vessel outlet side. The potential life was also estimated considering a safety residual length of 40mm and the maximum wear rate obtained. Table 2 summarizes the results.

Table 2. Wear rate and potential life of customer B lower vessel outlet side.

Wear rate (mm/heat)		Potential life (heats)
Average	Maximum	
1.16	1.80	144

For comparison purposes, Table 3 shows the average and maximum wear rates as well as the potential life of two other vessels assembled with tempered $MgO\text{-}Cr_2O_3$ bricks over the same period as the previous one. The calculations consider the same conditions: initial length of 300mm and safety residual length of 40mm.

Table 3. Wear rate and potential life of two other vessels in customer B.

Life (heats)	Wear rate (mm/heat)		Potential life (heats)
	Average	Maximum	
140	1.36	1.41	185
113	0.99	1.86	140

For all three vessels, the lowest potential life is close to the RH life goal set by the customer, which is currently 140 heats. This indicates the suitability for regular supply in this customer as well.

2.2.2. Post-mortem analysis

Post-mortem analysis of the sample selected from customer B was done. The sample was divided into three distinct regions: hot face (HF), intermediate zone (IZ), and cold face (CF), and the analysis below were carried out in each one of them. Chemical analysis was done by X-ray fluorescence in the MagiX Pro (Philips) equipment using SuperQ database. Bulk density (BD) and apparent porosity (AP) were measured according to ASTM C20. Optical microscopy was analyzed in the Carl Zeizz (AXIO-Imager) equipment.

The initial dimensions of the brick were: 300mm long, 100mm high, 170mm wide on the cold face, and 130mm wide on the hot face. Figure 12a shows the final dimensions of the brick, the shortest length was 77 mm, which is slightly different from the RBL shown in Figure 11, due to the different measurement conditions in the lab and in the field. Figure 12b shows the cross session of the material and no infiltration is observed, only a thin layer of adhered slag to the brick surface.

Figure 12. Post mortem sample (a) dimensions and (b) cross session.

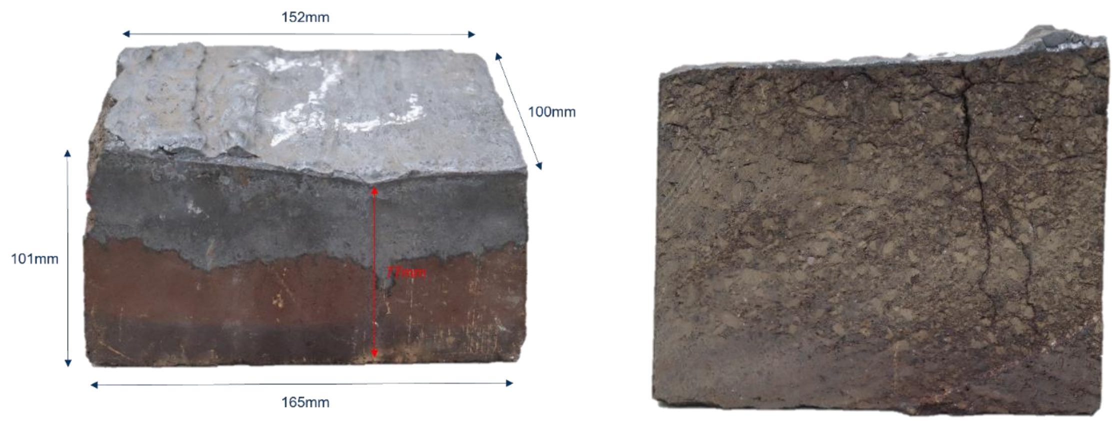

(a) (b)

Table 4 shows the chemical analysis and physical properties of the three defined zones of the used tempered $MgO-Cr_2O_3$ brick.

Table 4. Chemical analysis and physical properties of the post-mortem sample.

	HF	**IZ**	**CF**
Chemical analysis (%)			
MgO	62.28	62.86	63.23
Cr_2O_3	19.38	19.07	19.04
Fe_2O_3	9.61	9.04	9.22
Al_2O_3	4.85	4.71	4.86
CaO	1.90	1.84	1.67
SiO_2	1.65	2.14	1.38
TiO_2	0.14	0.18	0.13
Physical properties			
Bulk density (g/cm^3)	3.30	3.31	3.30
Apparent porosity (%)	12.85	12.60	12.85

Both the physical properties and the chemical composition of the material hardly vary between the three evaluated regions. This can be explained by the fact that the special binder increases the system reactiveness, thus the whole brick is able to develop its microstructure, leading to similar physical properties throughout it. The nearly homogeneous chemical composition, on the other hand, indicates the absence of infiltration into the material.

Figures 13a, 13b, and 13c show the optical microscopy of the hot face, intermediate zone, and cold face, respectively. The hot face has a densified layer and from there on it is possible to observe the material sintering, the direct bonding formation between the grains, and the secondary spinels formation. These spinel-like phases are extremally important against corrosion as they accommodate slag elements in their structure, thus avoiding corrosion mechanisms[8].

Figure 13. Optical microscopy of the post-mortem sample: (a) HF, (b) IZ, and (c) CF.

1: Densified layer; 2: Fused magnesia-chromite; 3: Chromite; 4: Pore.

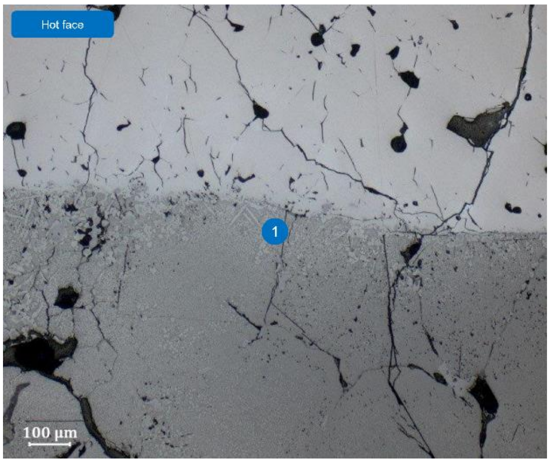

(a)

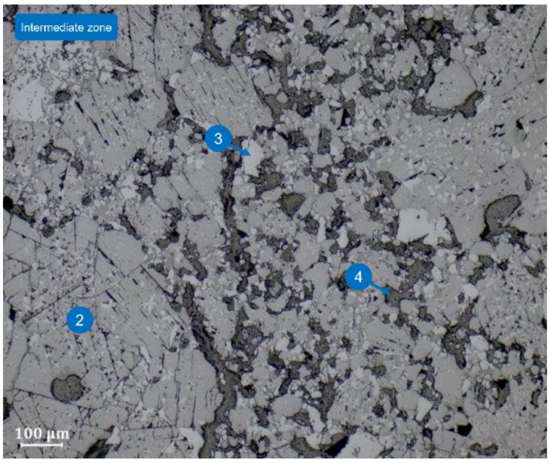

(b)

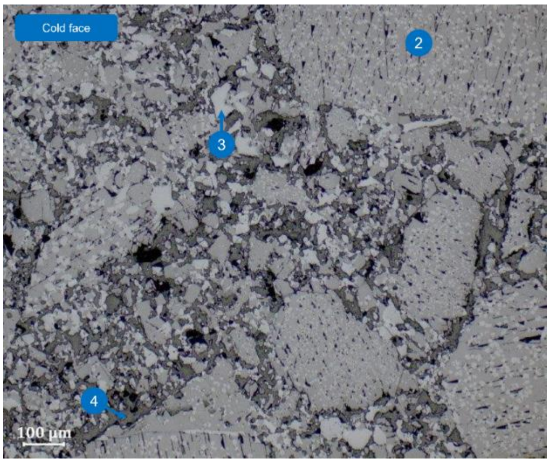

(c)

3. CONCLUSIONS

Tempered MgO-Cr_2O_3 brick with unique binder system was developed for application in RH Degasser lining. Its fast-sintering ability allows it to be delivered to the customer only tempered at 200 °C, thus reducing the material carbon footprint and lead time, which is important in times of supply chain disruption.

Field trials were conducted in the past and presented in previous works[1,6,7], leading to routine use of the material in some Brazilian customers. In customer A tempered MgO-Cr_2O_3 material had an outstanding performance reaching 170 heats, which is the mill record. In customer B the material also had good performance and its post-mortem analysis showed excellent resistance against the main wear mechanism for this application.

REFERENCES

1 Biswas, S.; Sarkar, D. **Introduction of refractories for Iron-and Steelmaking**. Switzerland, Springer International Publishing, 2020.

2 Borges, B.; Pagliosa, C.; Borges, M.; Campos, A.; Madalena, V. **Zero Carbon Tempered MgO-Cr2O3 for RH Degassers: Advances from Customers' Trials**. UNITECR, 2022.

3 Lee, W. E.; Zhang, S. **Melt corrosion of oxide and oxide-carbon refractories**. International Materials Reviews, v. 44, n. 3, p. 77–104, 1999.

4 Ferreira, L. L. H. C. **Desenvolvimento de agregados eletrofundidos para utilização em refratários para a zona de queima de fornos de cimento**. Tese apresentada como parte dos requisitos para obtenção do Grau de Doutor em Ciências na Área de Tecnologia Nuclear, Instituto de Pesquisas Energéticas e Nucleares, IPEN, Autarquia Associada à Universidade de São Paulo, São Paulo, 2006.

5 Czapka, Z.; Skalska, M.; Zelik, W. **Mechanism of wear of refractory materials in snorkels of RH degasser and the possibilities for their reduction**. UNITECR, 2005.

6 Pagliosa, C.; Campos, A.; Borges, B.; Madalena, V.; Pandolfelli, V.C. **Novel Tempered MgO-Cr_2O_3 Bricks with Zero C Binder for RH Degasser**. UNITECR, 2019.

7 Pagliosa, C.; Borges, B.; Campos, A.; Borges, M.; Avila, H.; Verona, M.; Madalena, V. **Tempered Magnesia Chrome Refractory Brick: Customers Trials Highlight**. ABM Week, 2022.

8 Berjonneau J.; Prigent P.; Poirier J. **The development of a thermodynamic model for Al_2O_3–MgO refractory castable corrosion by secondary metallurgy steel ladle slags**. Ceramics International, v. 35, n. 2, p. 623–635, 2009.